Exchange coupling with the multiferroic compound $BiFeO_3$ in antiferromagnetic multidomain films and single-domain crystals

D. Lebeugle,[1,2] A. Mougin,[1,*] M. Viret,[2] D. Colson,[2] J. Allibe,[3] H. Béa,[3] E. Jacquet,[3] C. Deranlot,[3] M. Bibes,[3] and A. Barthélémy[3]

[1]*Laboratoire de Physique des Solides, Université Paris-Sud, CNRS, UMR 8502, Bâtiment 510, 91405 Orsay, France*

[2]*CEA Saclay, DSM-IRAMIS-SPEC, Orme des Merisiers, 91191 Gif-sur-Yvette, France*

[3]*Unité Mixte de Physique CNRS-Thales, Route Départementale 128, 91767 Palaiseau, France*

(Received 24 September 2009; revised manuscript received 9 February 2010; published 8 April 2010)

The exchange coupling observed between a soft ferromagnetic layer and the antiferromagnetic multiferroic compound $BiFeO_3$ (BFO) is investigated. Results obtained on BFO ferroelectric and antiferromagnetic multidomain films and monodomain single crystals are compared. A significant interface coupling occurs in the two systems whose anisotropy however differs significantly. In thin film based heterostructures, the measured twofold anisotropy of the FM layer imposed by the magnetic field during deposition is well accounted for using a double macrospin model describing the role of uncompensated spins, pinned or reversible, in the vicinity of the interface. In contrast, no macroscopic bias is observed in thin films deposited on BFO single crystals where the anisotropy direction is imposed by the underlying antiferromagnetic structure. This highlights the fundamental difference between exchange coupling with a single domain antiferromagnet and with a much more magnetically disordered multidomain state.

DOI: 10.1103/PhysRevB.81.134411 PACS number(s): 77.84.Bw, 75.30.Et, 77.80.Dj, 75.50.Dd

I. INTRODUCTION

The bifunctionality of some multiferroic materials,[1–3] which present simultaneous ferroelectric (FE) and magnetic orders, is a property of a great interest for new potential devices for spintronics and in magnetic data storage applications. Indeed, controlling the magnetization of a ferromagnetic (FM) or an antiferromagnetic (AFM) layer with electric fields via the so called "magnetoelectric coupling" interaction would allow the conception of electrically writable and magnetically readable memories.[4] As ferroelectric materials are seldom ferromagnetic and more often antiferromagnetic, addressing a net magnetization with an electric field could be done combining the magnetoelectric coupling between antiferromagnetism and ferroelectricity with the exchange coupling at the interface between a FM and an AFM-FE multiferroic layer.[5–7] Among all multiferroics, $BiFeO_3$ (BFO) is the only one at room temperature. Its AFM (T_N=643 K in the bulk[8]) and FE (T_C=1143 K in the bulk[8]) ordering temperatures are well above room temperature. Since its discovery in 1956,[9,10] the exchange coupling between a FM and an AFM has provided an important research activity in magnetism along with challenges to the understanding of interfaces between magnetic materials. Among the experimental signatures associated with magnetic coupling through this interface, the most obvious is a change in the coercivity and a shift or "bias" of the FM layer's magnetization hysteresis loops. An overwhelming literature has emerged in which various mechanisms for this coupling have been proposed, debated, and tested (for reviews, see Refs. 11–13). One of the key aspects of this problem is the relation between domains, domain walls, pinned or reversible uncompensated spins in the AFM and coercivity or bias in the FM. The first point addressed in this paper is that of the strength of the exchange bias field. An exchange bias field exists in CoFeB or NiFe layers deposited on BFO thin films,[7,14,15] but this bias was never discussed in heterostructures based on single crystals, in which a modulated long-range AFM structure strongly coupled to the polarization, has been evidenced at room temperature.[16] Indeed, one can in principle learn a great deal about ordering processes in the AFM by observing the FM magnetization reversal and anisotropy in such coupled structures. In many exchange coupled crystalline AF or F systems, the specific directions of the AFM vectors of the crystal are visible in the exchange coupling properties. However, this is not always the case and it still remains unclear whether the AFM arrangement, in these systems, survives exactly all the way to the interface. This is the second and main purpose of this paper, in which we compare the magnetic behavior of heterostructures constituted of a ferromagnetic films deposited on BFO in single crystal and as thin film forms. A significant interface coupling occurs in the two systems whose anisotropy, however, differs significantly. In thin film based heterostructures, a twofold anisotropy of the FM layer is evidenced, which does not depend on the particular directions of the BFO antiferromagnetic structure. Interestingly, no macroscopic bias is observed in NiFe films deposited on BFO crystals where the anisotropy direction is found to be imposed by the underlying antiferromagnetic structure. We will also comment on preliminary experiments revealing the possibility to locally control ferromagnetism with an electric field using $BiFeO_3$ as the multiferroic layer[6,17] or the electric-field induced modification of the FM anisotropy using $BiFeO_3$ crystals published recently.[18]

II. SAMPLE'S PROPERTIES

A. Single-domain BFO crystals

Using a flux technique, high quality millimeter sized BFO single crystals were synthesized.[19] The crystal-bulk like present a noncentrosymmetric pseudocubic cell with a rhom-

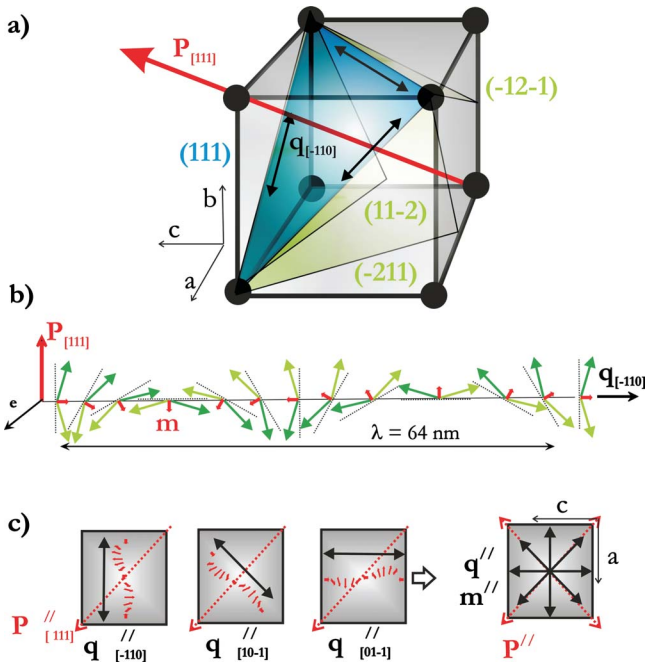

FIG. 1. (Color online) Orientation and projections of the polarization P and the magnetic moments in single-domain crystals of $BiFeO_3$. (a) Representation in the pseudocubic system of the (111) plane containing the three possible $\langle 101\rangle$ cycloid propagation vectors assuming a polarization P along [111] in a single crystalline platelet of BFO. The magnetic moments are contained in one of the {121} planes. (b) Sketch of the magnetic moments M (long arrows) forming a cycloid in the $(11\bar{2})$ plane; the moments depicted by the dark or light arrows illustrate the AF coupling from one plane to the next. Due to the canting, the induced local moment m (shorter and broader arrows) is zero over a modulation period. (c) On the (010) plane covered by the ferromagnet, from left to right: For P along [111] ($P_{[111]}$) and for q parallel to $[\bar{1}10]$ ($q_{[\bar{1}10]}$), the projection of the canted moment m is modulated along [100]; it is along the diagonal [101] for $q_{[10\bar{1}]}$ and along [001] for $q_{[01\bar{1}]}$. Taking into account all possible orientations of the polarization in the single crystal among the eight $\langle 111\rangle$ ones, projection of m on the surface plane modulated along the $\langle 100\rangle$ or $\langle 110\rangle$ directions, imposed by the propagation vector.

bohedral distortion (a=3.96 Å and α=89.4°). As grown, most crystals are FE and AFM single domains.[16] They are also highly resistive and the value of the electric polarization at saturation $P_S \approx 100\ \mu C/cm^2$ turns out to be the highest known so far.[20] In bulk BFO, the polarization lies along the $\langle 111\rangle$ directions, allowing for eight possible polarization variants leading to eight possible ferroelectric domains. Crystals are FE single domains and the polarization P is along one of the $\langle 111\rangle$ direction (Fig. 1). Using four-circle neutron measurements, we demonstrated that the magnetic configuration is closely linked to the electric state of the crystals with a strict correspondence between the FE and the AFM domains.[16] It was demonstrated that the AFM structure is cycloidal G-type: for P parallel to [111], coupled nearest-neighbor Fe^{3+} moments are arranged in a long period (64 nm) cycloid in one of the plane of {121} character (Fig. 1).[16] The plane containing the magnetic moments M contains the electric polarization P and the cycloid propagation vector q. The latter, perpendicular to the electric polarization direction, has three possible orientations: it is along one of the $\langle 110\rangle$ directions contained in the (111) plane for $P_{[111]}$ [Fig. 1(a)]. An antiferromagnetic coupling is observed from one {121} plane to the next. Choosing a propagation vector, q along, e.g., $[\bar{1}10]$ imposes the magnetic plane $(11\bar{2})$. A canting of the Fe^{3+} moments results in a local moment m, rotating from one site to the next and whose average over the cycloidal modulation vanishes: this peculiar arrangement is sketched Fig. 1(b). For a single crystal being a FE and AFM single domain, whatever the direction of the polarization among the eight possible ones, the weak moment m resulting from the canting is modulated along the in-plane $\langle 110\rangle$ or $\langle 100\rangle$ directions [Fig. 1(c)] when projected onto the (010) plane. The projection of this weak moment m has different strength, depending on the propagation vector: it is larger for $q_{[10\bar{1}]}$, included in the (010) plane, than for the two other propagation vectors making an angle of 45° with the interfacial plane. In all cases, the top ferromagnetic layer will interact with a long scale modulated magnetic structure, showing no global ferromagnetic moment, assuming that the "bulk" structure is preserved in BFO or FM systems described later. The orientation of the modulation is that of the projection of the propagation vector of the AFM ellipsoid.

B. Multidomain BFO thin films

BFO films were epitaxially grown by pulsed laser deposition on (001) $SrTiO_3$ (STO) substrates at $P=10^{-2}$ mbar and T_{dep}=580 °C. At lower temperature or higher pressure, Bi_2O_3 precipitates appear while at lower pressure or higher temperature, Fe_2O_3 forms. Magnetization measurements reveal a high magnetic moment for films containing γ-Fe_2O_3 impurities while single-phase films have a very low but not zero magnetic moment ($\sim 0.02\mu_B$/f.u.).[21,22] No information is available on the spatial arrangement of that small amount of uncompensated moments, reversing at low magnetic field, in the BFO films. The BFO (001) films present a noncentrosymmetric pseudocubic cell with a tetragonal distortion (a=3.78 Å and c=4.85 Å). A value of the electric polarization P is inferred from P-E loops measurements and the saturation polarization estimated to $P_S \approx 100\ \mu C/cm^2$, like in crystals. From neutron-diffraction experiments,[14] it was demonstrated that the AFM structure is collinear G-type with the Fe^{3+} AFM moments located in the {111} easy planes [Fig. 2(a)]. In thin films, the {111} antiferromagnetic planes are arranged perpendicularly to the ferroelectric polarization P along the relevant $\langle 111\rangle$ directions; the characteristic propagation vector of the AFM structure remains here parallel to the electric polarization. Up to now, no consensus has been achieved to lift the degeneracy between all directions within the {111} planes that can be considered as effective easy planes of magnetization. As grown, the BFO thin films where shown to be in a ferroelectric multidomain state, which also imposes AFM domains, whose size (of the order of a few tens of nanometers) increases with the layer thickness.

Let us now discuss on the magnetic structure at the interface between the CoFeB and the BFO films. First, starting with an *a priori* uncompensated AF structure in the {111}

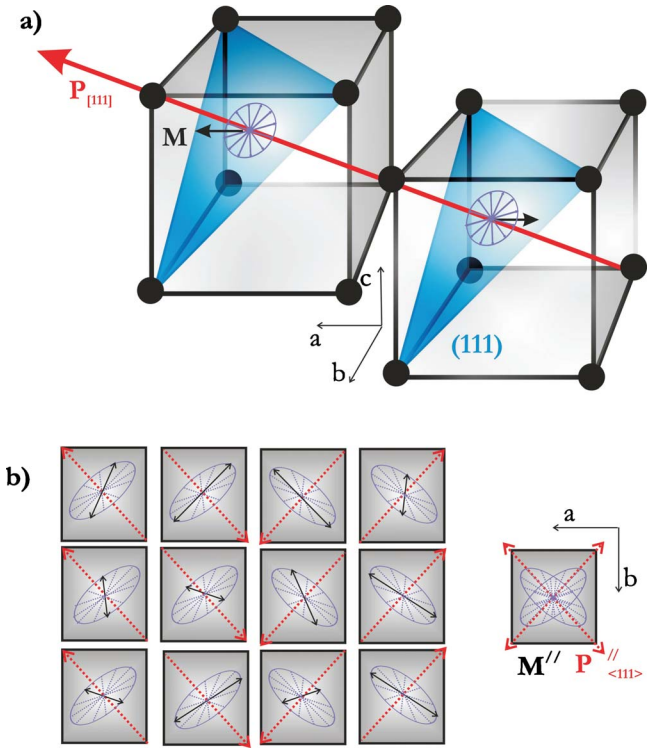

FIG. 2. (Color online) Epitaxial BFO films on (001) $SrTiO_3$ (STO) and projections. (a) Representation in the pseudocubic system of the {111} easy magnetization plane of a single AFM domain in a thin films of BFO. The (111) magnetic planes are perpendicular to the spontaneous polarization P, depicted here along [111]. No preferential orientation is expected for the magnetization within the (111) plane, as sketched by the circular rotative arrow whereas an antiferromagnetic coupling is imposed from one plane to the next. (b) Collection of ten possible individual AFM domains. In each case, the orientations have arbitrary chosen. The dotted arrows depict the projection of the electric polarization on the (001) plane, always along ⟨110⟩ directions. The black arrows correspond to the projection of the magnetic moments whose strength is imposed by the orientation of the spin in the {111} planes. The isolated drawing, giving rise to twin elliptical-like structures, rotated by 90° one from another, results from the averaging of the entire set of possible coupled projections for P and M.

planes, this magnetic structure is compensated when projected on the (001) interfacial plane. The magnetic moments can be oriented along any direction of the easy {111} plane, and their projection on the (001) plane can be along any axis of the ellipsoid depicted in Fig. 2(b). The later merges a nonexhaustive set of possible orientations and projections of P and M. Depending on their orientation within the (111) plane, the projection of individual moments varies in strength: it has maxima when M is aligned along ⟨110⟩-type directions within {111} planes since the projection of M makes then an angle of 90° with that of the polarization's projection. On the contrary, the projection of M is minimum along the polarization's projection. At the scale of an AFM single domain, the interfacial structure mimics a twofold anisotropy axis. At the much larger scale of a ferromagnetic domain in the CoFeB layer, the magnetic local structure has to be averaged over several AFM domain configurations. Then, taking into account the eight possible orientations of the polarization along the ⟨111⟩ directions, in the (001) plane, the projection of the underlying magnetic structure gives rise to two ellipticlike patterns elongated along ⟨110⟩ directions at 90° one from another. From a macroscopic point of view, the top FM layer feels this not fully isotropic repartition of the compensated interfacial magnetic moments.

C. Comparison with reference to bias and samples details

There are four important differences between BFO in bulk and thin film form: the single domain or multidomain state, the cycloidal or collinear G-type AFM structure, the absence or existence of a ferromagnetic moment and the fixed along main crystallographic directions or twinned elliptical projection of the magnetic moments embedded in the AFM structure onto the interfacial plane. The last points are of major importance for the exchange bias problem. Indeed, magnetic properties of the FM film in contact are attributed to a net magnetization in the AFM close to the interface due to the presence of pinned, or not, uncompensated spins and related to all imperfections including domain walls, atomic steps, interface roughness, and atomic-scale disorder.[23–27] Nowadays, most of the experimental and theoretical studies concerning the exchange bias tend to show that the bias field is due to a pinned ferromagnetic component in the AFM layer, close to the interface[26,27] and is related to the formation of domain walls perpendicular[28] or parallel[29] to the interface in the AFM layer. It then appears that the exchange bias is not a purely interfacial property but the domain configuration of the AFM layer also has to be taken into account. In an attempt to clarify the mechanisms of exchange bias in our BFO-based structures, we propose here to compare results obtained on FM deposited on BFO thin films and single crystals. Studying the angular dependence of H_E and H_C sheds some light on the nature of the exchange coupling in the two systems and the strength of the AFM and FM anisotropies. Two standard behavior will be kept in mind as references: in usual polycrystalline systems of FM (without any intrinsic anisotropy) or AFM, the exchange bias field presents a sinusoidal angular dependence with maxima (respectively, minima) of coercivity and bias along (respectively, perpendicular to) the applied field used to set the bias whereas epitaxial systems with strong magnetocrystalline anisotropy often exhibit a complex dependence[30] with very asymmetric hysteresis loops.[31,32]

The structures of the present study are of two types. First, they consist in a 10 nm ferromagnetic layer of polycrystalline Permalloy Py sputtered onto the (010) plane of ferroelectric and antiferromagnetic single-domain BFO crystals, after a short etching. No quantitative information is available at small scale about the structural interfacial roughness of the systems. However, from optical experiments, it can be asserted that some micrometric steps exist that spread laterally over several micrometers separating flat terraces. We do not have any direct evidence for the existence of the cycloids at the surface of our BFO crystals before deposition. However, the direction of the anisotropy that we measure in the FM layer can be taken as indirect evidence for their survival all

the way to the interface.[18] We will come back to this point in the discussion of our results. During the FM layer deposition, a magnetic field H_{dep} of magnitude 200 Oe is applied in the (010) plane of BFO crystal's platelet. A thin layer of Au (4 nm) is also sputtered as a protection layer. Second, the other studied structures consist in a ferromagnetic layer of CoFeB (7.5 or 5 nm) deposited on BFO(35 nm) or STO(001) films. Indeed it has been reported recently that BFO films can be used to induce an exchange bias on adjacent CoFeB layers at 300 K.[7,14] The amorphous FM CoFeB layers are sputtered in a separate chamber in a 200 Oe magnetic field H_{dep}, after a short plasma cleaning. Neutron reflectivity measurements showed that the structural interfacial roughness in BFO or FM heterostructures is about 0.5 nm. This demonstrates that the etching process performed just before deposition of the ferromagnet does not significantly damage the surface quality. However, the etching may alter the magnetic structure of the BFO close to the surface since it was shown that a 2-nm-thick magnetic roughness had also to be taken into account in the vicinity of the interface that contains uncompensated spins, among which only 1% are pinned.[14] A thin layer of Au (4 nm) is also deposited as a protection layer.

III. EXPERIMENTAL RESULTS AND DISCUSSION: FILMS VERSUS CRYSTALS

The longitudinal FM magneto-optic Kerr effect (MOKE) hysteresis loops were measured at room temperature as a function of the angle between the applied field H and BFO main axis, in crystals and films based bilayers. The loops collected for a complete rotation, with 5° steps, were analyzed in terms of coercivity, bias, and shape. Different orientations have been also used for testing the influence of the orientation of the deposition field H_{dep}, in reference to the BFO main axis.

A. Single BFO crystals

Figure 3(a) shows typical FM loops along the easy axis and along the hard axis of the Py layer. No noticeable shift of the FM loop is observed evidencing the absence of bias field in the crystals. Similar results have been obtained with CoFeB as the ferromagnet. However, because the macroscopic exchange bias field is inversely proportional to the saturation magnetization of the FM layer, we focused on NiFe which has lower magnetization than CoFeB, thus allowing for a larger sensitivity for testing small bias fields. Despite this, we measure strictly no bias. However, the loops are enlarged compared to those measured on similar Py films deposited in the same runs on floated glass, as a reference sample. This observation is the signature of a significant exchange coupling between the two layers, despite the absence of macroscopic bias. Figure 3(b) shows the angular dependence of the remanence and switching fields as a function of the direction of the applied magnetic field H, in polar representation. H_E being zero in the entire range of angles in the Py or BFO crystal system is not represented. Moreover, in the single crystals, as the coercive field is not always well defined because of the contribution of the transverse magnetization, it is instructive to plot the switching field—defined as the saturation field—instead of the usual coercive field, as well as the remanence. In these conditions, the maximum of the switching field, respectively, minimum of the remanence, gives the hard axis that is the [001] direction (indeed the switching of the transverse magnetization occurs when the magnetic field is applied near the hard axis), whereas the secondary maximum of H_{switch}, respectively, the maximum of the remanence, gives the easy axis that is the [100] direction. It is important to note is that the field applied during deposition H_{dep} was applied at 20° from the [100], i.e., on purpose misaligned relative to the major crystallographic directions in the FM or BFO crystal shown in Fig. 3(b). Additional experiments made on bilayers grown with different orientations of H_{dep} lead to the conclusion that in the Py or BFO crystal (antiferromagnetic monodomain), the coercivity presents two maxima independent of the deposition field and that no bias field is measured. On the contrary, the easy axis

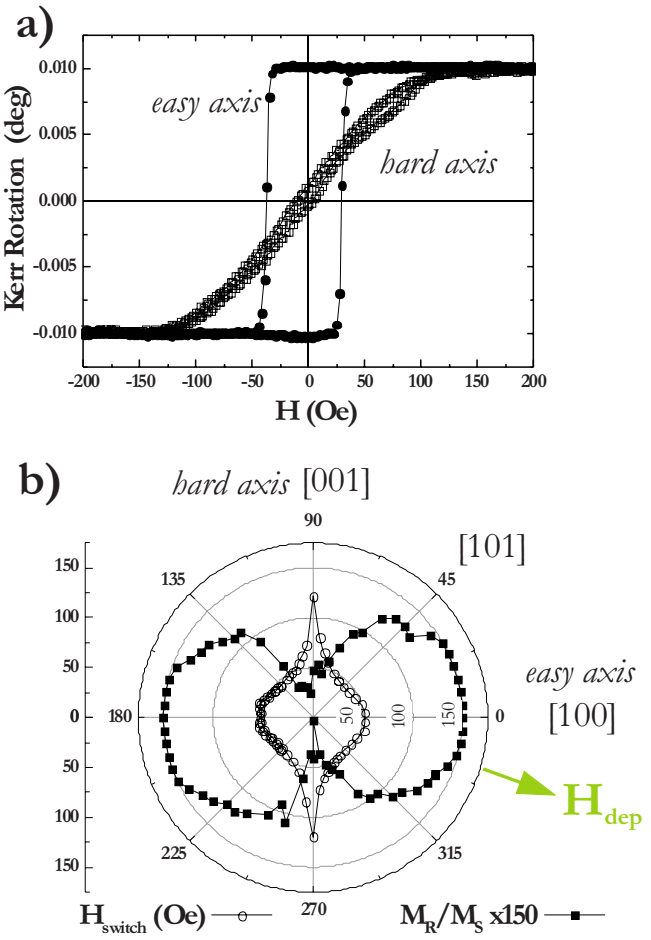

FIG. 3. (Color online) (a) Longitudinal ferromagnetic hysteresis cycle (MOKE) of a Permalloy layer deposited on a single-domain BFO crystal: along the easy direction (dots) and along the hard direction (squares). (b) Polar plot of the evolution of M_R/M_S and H_{switch} of a Py or single-domain BFO crystal. For readability, values are added on the circle lines in addition to the usual vertical scale. The angle is defined between the applied field H and the [100] direction of BFO. The deposition field $\vec{H}_{dep}$ is represented by the large arrow.

of the reference Py layer on glass is always parallel to that field applied during deposition H_{dep}, as expected. Hence, we show experimentally that the induced anisotropy in the FM layer is not related to how the deposition field is aligned but that the easy axis is always along one of the major axes of the BFO crystals, [100], [001], or [110].

Now, we discuss the lack of bias and the coercivity response in the Py or BFO crystal system. For the BFO single crystals, the presence of the cycloid makes the magnetization fully compensated in the interfacial plane (010). If no bias is expected in perfect compensated systems, it has been reported that a bias can arise when uncompensated and irreversible spins exist, whose origin is usually discussed in relation with defects and domains walls. Here, the lack of bias is fully consistent with the argument "the larger the bias, the larger the amount of domains walls" since our crystal are in a single domain state, with no walls. The experimental observations relative to the coercivity can be discussed taking into account the presence of compensated free spins with weak anisotropy leading to no bias but to an enhancement of the coercive field. The pseudotwofold anisotropy observed in the angular coercivity response can be attributed to the exchange coupling with the magnetic structure sketched in Fig. 1(c). At the interface, the exchange energy between the ferromagnet and the projection of the canted moment that describes the cycloid is locally not zero. Due to the period of the cycloid of the order of a few exchange lengths of the Permalloy layer, the ferromagnet is not likely to follow exactly this specific arrangement but the exchange coupling should induce a wriggling of the ferromagnet's magnetization along the propagation vector of the underlying cycloid [see Fig. 1(c)]. A ferromagnet's ripple can be established, distributed laterally with a periodicity determined by the exchange length of the ferromagnet. As usually, the wavelength of the fluctuations drives the formation of high-order terms in the effective energies. We argue that the demagnetizing energy of the heterostructure FM or BFO crystal is smaller when the ferromagnet's magnetization is in overall parallel with the propagation vector of the cycloid whereas it is larger when perpendicular to it. This results in an induced pseudotwofold anisotropy in the ferromagnet, imposed by the propagation vector of the BFO cycloidal structure. The mechanism of this induced anisotropy has been supported by additional investigations under the application of an electric field, reported in more details elsewhere.[18]

B. Multidomain BFO thin films

As said, exchange bias has already been observed in such system.[7,14] From neutron scattering and piezoresponse force microscopy, it was shown that the macroscopic exchange bias field in CoFeB or BFO heterostructures scales with the inverse of the FE or AFM domain size of the BFO films, as expected from Malozemoff's model of exchange bias extended to multiferroics. The observation of uncompensated spins at the interface by polarized neutron reflectometry (PNR) correlates with this model.[14] Figure 4(a) shows typical CoFeB loops along the easy and hard axis for a CoFeB thickness of 7.5 nm. The macroscopic shift H_E of the FM

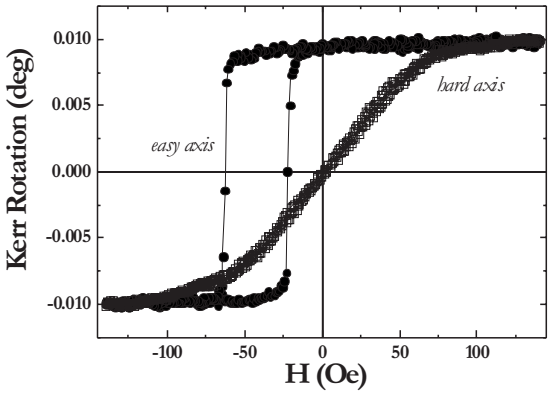

FIG. 4. Longitudinal ferromagnetic hysteresis loop (MOKE) of a CoFeB layer deposited on a BFO or STO film along the easy (dots) and hard (squares) directions.

loops is one of the signatures of exchange-bias in these bilayers; another one is the enlargement of the coercivity H_C by about 70% compared to those measured on reference CoFeB thin films.

Figure 5(a) shows the angular dependence of the bias and coercive fields as a function of the direction of the applied magnetic field H for three orientations of H_{dep} in CoFeB/BFO(001) bilayers. The deposition field has been applied along major crystallographic directions ([001] and [110]) of the BFO film and on purpose misaligned by 20° from the main directions [Fig. 5(a), middle plot]. In this last case, the thickness of the ferromagnetic layer has been decreased to 5 nm which results in larger bias and coercive fields.[14] The loops are shifted toward negative magnetic field values by an exchange field of about −40 Oe for 7.5-nm-thick CoFeB layers [Fig. 4(a)] and it is increased to −60 Oe for a reduced thickness of 5 nm, confirming former results indicating an inverse proportionality relationship between the ferromagnet thickness and the bias field. In Fig. 5(a), one sees that H_E and H_C have extrema along H_{dep}, irrelevantly of whether this direction is along a high symmetry or not. At first sight, this angular dependence looks like a unidirectional induced anisotropy in the CoFeB layer along the deposition field. However, as this can be seen from the details of Fig. 5(a), the dependence of the bias field is not a pure sinusoid. It exhibits a rounding and two kinks at 135 and 225° around the deposition field axis. The deviation from a simple sine behavior is even more obvious for the coercive field that differs from zero over a large range of angles around H_{dep}, whereas a peaked behavior is expected in bilayers showing a typical unidirectional response.

It is known that in some epitaxial FM or AFM bilayers, H_E is far from being a simple sine dependence centered on the field cooling direction, in contrast to what was initially postulated for polycrystalline samples.[9,10] One way used to reproduce the angular behavior of the ferromagnet is to add phenomenological high-order anisotropy terms in a Stoner-Wohlfarth-type model, entering the FM energy.[30] However, this approach considers implicitly the AFM as frozen. In order to reproduce the observed angular dependence in CoFeB/BFO(001) bilayers, we modeled them by taking into account the CoFeB film's magnetization ($\vec{M}^F$), a net magnetization

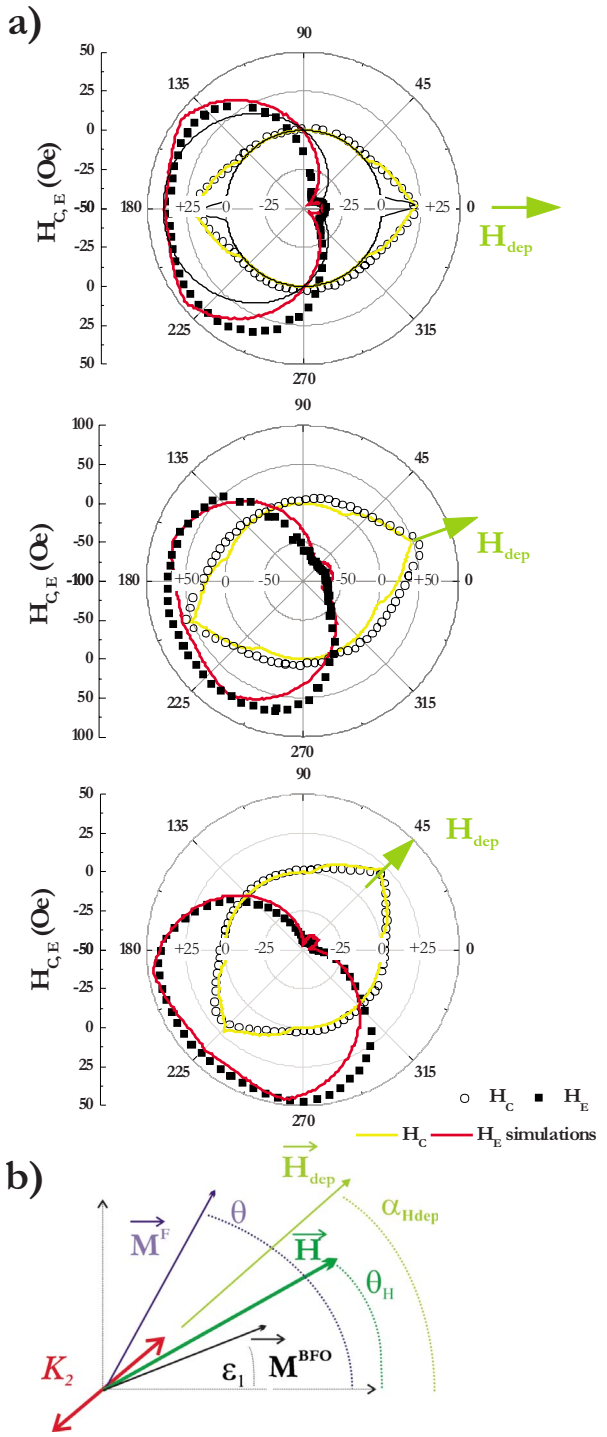

FIG. 5. (Color online) (a) Polar plot of the evolution of H_E (squares) and H_C (open circles) in a CoFeB/BFO (001) heterostructures, field grown. The angle is defined between the applied field and the [100] direction of BFO. For readability, values are added on the circle lines in addition to the usual vertical scale. The deposition field $\vec{H}_{dep}$ is represented by a large arrow. For comparison, the bias field and the corresponding coercive field when assuming a sine dependence for the unidirectional exchange coupling are shown by black solid lines. The wide gray solid lines are the results of the model described in the text. (b) Magnetization vectors $\vec{M}^F, \vec{M}^{BFO}$, deposition $\vec{H}_{dep}$ and applied $\vec{H}$ fields, angles and anisotropies in the simulations of CoFeB/BFO(001) bilayers.

($\vec{M}^{BFO}$) assigned to the BFO layer, the interfacial exchange (noted J) between them and one twofold magnetic axis (K_2) ascribed to the BFO layer, along the deposition field axis. No intrinsic or "hand" added anisotropy is assigned to the FM layer since it is amorphous. Exchange bias is represented by a field $\vec{h}^{pinned}$ along $\vec{H}_{dep}$ that acts as an additional field on the magnetization. We assume that this field results from pinned uncompensated spins, close to the interface between the BFO and CoFeB films.[24,27,33] All vectors and angles involved in the modeling are sketched in Fig. 5(b). The orientation of $\vec{M}^F$ is defined by θ that of $\vec{M}^{BFO}$ by ε, whereas $\vec{H}^{dep}$ and $\vec{H}$ are defined by θ_H and α_{dep}, respectively. The equilibrium state during magnetization reversal corresponds to a minimum of the free energy, expressed by the vanishing of the torque $\vec{M} \times \vec{H}_{eff}$ where the effective field $\vec{H}_{eff}$ obeys $\vec{H}_{eff} = -\frac{\partial G}{\partial \vec{M}}$. The free-energy density [Eq. (1)] is defined as

$$G = -\vec{M}^F \cdot [\vec{H} + \vec{h}^{pinned}] - J\frac{\vec{M}^F \vec{M}^{BFO}}{M^F M^{BFO}} - K_2^{BFO} \cos^2(\varepsilon - \alpha_{dep}). \tag{1}$$

The effective field components $H^F_{eff,(x,y)}$ in the (x,y) directions acting on the ferromagnet F are given by Eq. (2):

$$H^F_{eff,x} = H \cos\,\theta_H + h^{pinned} \cos\,\alpha_{dep} + \frac{J}{M^F}\cos\,\varepsilon,$$

$$H^F_{eff,y} = H \sin\,\theta_H + h^{pinned} \sin\,\alpha_{dep} + \frac{J}{M^F}\sin\,\varepsilon. \tag{2}$$

One notes that $\vec{H}^{pinned}$ can introduce a loss of symmetry in the effective fields. Similarly, the effective fields acting on the BFO are given by Eq. (3):

$$H^{BFO}_{eff,x} = \frac{2K_2^{BFO}}{M^{BFO}}(\cos\,\varepsilon \cos^2\,\alpha_{dep} + \sin\,\varepsilon \cos\,\alpha_{dep} \sin\,\alpha_{dep}) + \frac{J}{M^{BFO}}\cos\,\theta,$$

$$H^{BFO}_{eff,y} = \frac{2K_2^{BFO}}{M^{BFO}}(\sin\,\varepsilon \sin^2\,\alpha_{dep} + \cos\,\varepsilon \cos\,\alpha_{dep} \sin\,\alpha_{dep}) + \frac{J}{M^{BFO}}\sin\,\theta. \tag{3}$$

This "double macrospin" model provides the field dependence of the angle of the two magnetization vectors (θ and ε) by finding the minimum energy orientation of both FM and AFM. Detailed shapes of hysteresis curves were calculated and examples are given in Fig. 6. It is possible to reproduce usual square hysteresis loops for $\theta_H = \alpha_{dep}$ without major overestimation of the coercive field (which is usually obtained when fixing the AFM in a single macrospin approach); at 45° of the deposition field orientation, the shifted but not coercive and asymmetric loop of the FM layer is also well simulated; the hard axis loop is well reproduced as well. The model successfully reproduces in all deposition field geometries the overall tendency of the bias and coercive fields

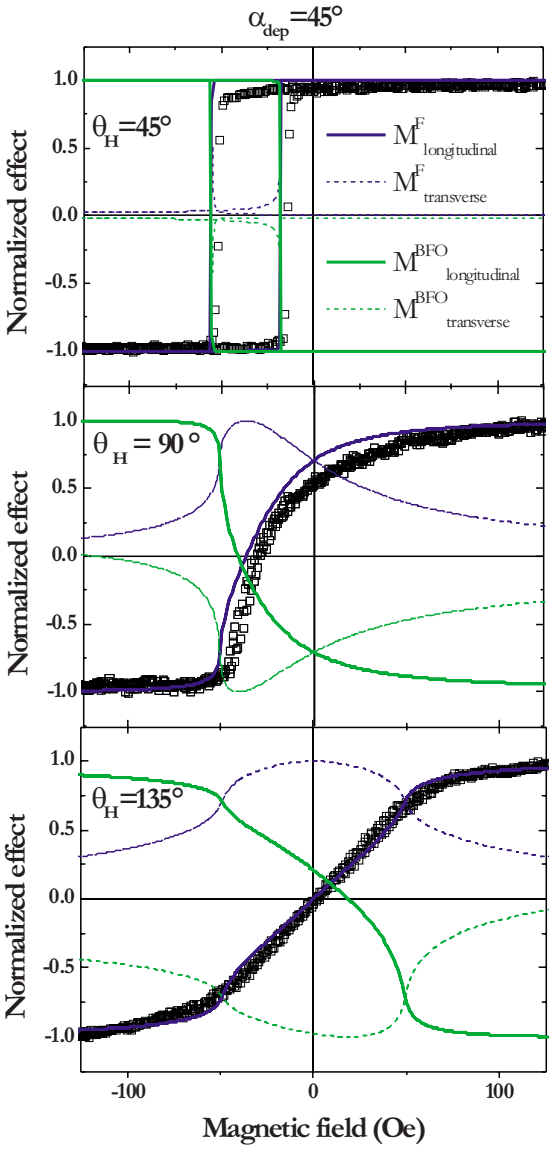

FIG. 6. (Color online) Longitudinal (along the applied field, continuous line) and transverse (perpendicular to the applied field, dotted line) hysteresis loops of M^F and M^{BFO} as measured (dots) and simulated (lines). Loops are obtained at 0° (easy axis) at 45° (intermediate direction) and at 90° (hard axis) from H_{dep}.

[Fig. 5(a)]. A single set of anisotropy and exchange fields was used for the bilayer's simulations: for BFO $K_2^{BFO}/M^{BFO}=13$ Oe and the interlayer exchange field $J/M^{\mathrm{CoFeB}}=J/M^{BFO}=45$ Oe. In these heterostructures, changing the orientation of $\vec{H}_{dep}$ from [110] to [001] only implied $|\vec{h}^{pinned}|=40$ Oe, whereas α_{dep} evolved from 0 to 45° in the simulations. To reproduce the larger bias and coercive fields obtained for a thinner CoFeB, the pinned field acting on the magnetization is taken as $|\vec{h}^{pinned}|=60$ Oe with α_{dep} equal to 20°.

Let us discuss the implication of strong coupling on the energy of Eq. (1). If J/K_2^{BFO} is small, $\varepsilon \approx \alpha_{dep}$, and the ferromagnet experiences no induced anisotropy since the AFM looks like frozen and no high-order anisotropy terms have been added in the FM energy. Likewise if J/K_2^{BFO} is larger than 1, $\varepsilon \neq \alpha_{dep}$ and the coupling J is large enough to cause large canting of the BFO surface magnetization away from its respective easy axis directions. As shown in Fig. 2(c), there is no intrinsic magnetic anisotropy in the BFO films and the twinned elliptical compensated spin arrangement stemming from the projection of the (111) easy magnetization plane onto the (001) interface is not far from isotropic. Therefore, we assumed the twofold anisotropy in the BFO as a consequence of the field deposition procedure. Then, the main features of the ferromagnet hysteresis can be interpreted as resulting from AFM spin rotation and an induced twofoldlike contribution appears in the ferromagnet because J/K_2^{BFO} is larger than 1. That is the way the system resolves the competition between local anisotropies and exchange coupling. This model does not include partial wall formation in the depth of the AF, whereas it is sometimes postulated that the high symmetry exchange anisotropy terms in the ferromagnet (i.e., its nonsinusoidal dependence relative to the deposition field orientation) originates from a partial AF wall parallel to the F or AF interface. Our "double macrospin" approach is therefore much simpler and is consistent with a model in which irreversible spins, whose directions can be set by the field initialization procedure, can be located, for instance, at the boundaries between the domains.

Usually, the initialization of the AFM in bilayers is done by a field cooling process through the Néel temperature of the AFM whose moments can orient in the field of the saturated ferromagnet, along the applied cooling field. Hence, here, we showed experimentally that the angular behavior of coercive field and exchange bias (in particular their extrema) are closely related to the deposition field direction. Moreover, the angular dependence of the exchange bias and the enhancement of the coercive field had to be related to a deposition field induced BFO anisotropy. The existence of a net moment in the BFO even if it is small, probably triggers the orientation of the BFO magnetic structure. The resulting magnitude of the coupling may be the limiting factor for future spintronics applications of the thin films.[15] In the crystals, where no net moment exists, the FM anisotropy is likely to result from the coupling with the underlying magnetic cycloid in the BFO.

IV. CONCLUSION

In summary, the comparison of the anisotropy of Py films on BFO monodomain crystals and of CoFeB or BFO multidomain films reveals a fundamental difference in the fingerprint of the BFO antiferromagnetic structures. The exchange coupling resulting from these two systems is of a completely different nature. In thin film based heterostructures, the magnetization is pinned in the vicinity of the bias field direction, whereas the anisotropy is driven by the AFM domain structure in single crystals. For multidomain films, our double macrospin model underlines the key role, in the FM magnetic response, of the rotation of the net magnetization in the BFO out of its anisotropy axis (induced by field deposition). It also puts forward the role of uncompensated spins, in agreement with former results on BFO thin films.[14,15] In Py or crystal systems, an induced anisotropy in the FM layer

along the propagation vector of the cycloidal arrangement of the antiferromagnetic BFO moments is observed irrelevantly of the presence and orientation of a field during deposition. The "bulk" BFO AFM structure is in that case the relevant parameter determining the FM properties thanks to a large effective exchange coupling. This is probably due to the strength of the magnetoelectric interaction inducing a larger local canting angle. The net moments, arranged in a long-range cycloid, couple to the ferromagnetic layer to induce a robust anisotropy. It was shown that an electric field induced change in electric polarization is able to toggle the easy direction of the ferromagnet through the magnetoelectric effect.[18,34]

ACKNOWLEDGMENTS

This work was supported by the Agence Nationale de la Recherche, Project "MELOIC" Grant No. ANR-08-NANO-040. Fruitful discussions with J. Camarero are also acknowledged.

*mougin@lps.u-psud.fr

[1] N. A. Spaldin and M. Fiebig, Science **309**, 391 (2005).
[2] W. Eerenstein, Science **307**, 1203 (2005).
[3] D. Khomskii, Phys. **2**, 20 (2009).
[4] M. Bibes and A. Barthélémy, Nature Mater. **7**, 425 (2008).
[5] T. Zhao *et al.*, Nature Mater. **5**, 823 (2006).
[6] V. Laukhin *et al.*, Phys. Rev. Lett. **97**, 227201 (2006).
[7] L. W. Martin, Y.-H. Chu, M. B. Holcomb, M. Huijben, P. Yu, S.-J. Han, D. Lee, S. X. Wang, and R. Ramesh, Nano Lett. **8**, 2050 (2008).
[8] R. Smith, G. Achenbach, R. Gerson, and W. James, J. Appl. Phys. **39**, 70 (1968).
[9] W. Meiklejohn and C. Bean, Phys. Rev. **102**, 1413 (1956).
[10] W. Meiklejohn and C. Bean, Phys. Rev. **105**, 904 (1957).
[11] A. Berkowitz and K. Takano, J. Magn. Magn. Mater. **200**, 552 (1999).
[12] J. Nogués and I. K. Schuller, J. Magn. Magn. Mater. **192**, 203 (1999).
[13] R. L. Stamps, J. Phys. D **33**, R247 (2000).
[14] H. Béa, M. Bibes, F. Ott, B. Dupé, X.-H. Zhu, S. Petit, S. Fusil, C. Deranlot, K. Bouzehouane, and A. Barthélémy, Phys. Rev. Lett. **100**, 017204 (2008).
[15] J. Dho and M. G. Blamire, J. Appl. Phys. **106**, 073914 (2009).
[16] D. Lebeugle, D. Colson, A. Forget, M. Viret, A. M. Bataille, and A. Gukasov, Phys. Rev. Lett. **100**, 227602 (2008).
[17] Y.-H. Chu *et al.*, Nature Mater. **7**, 678 (2008).
[18] D. Lebeugle, A. Mougin, M. Viret, D. Colson, and L. Ranno, Phys. Rev. Lett. **103**, 257601 (2009).
[19] D. Lebeugle, D. Colson, A. Forget, M. Viret, P. Bonville, J. F. Marucco, and S. Fusil, Phys. Rev. B **76**, 024116 (2007).
[20] M. Cazayous, D. Malka, D. Lebeugle, and D. Colson, Appl. Phys. Lett. **91**, 071910 (2007).
[21] H. Béa, M. Bibes, S. Fusil, K. Bouzehouane, E. Jacquet, K. Rode, P. Bencok, and A. Barthélémy, Phys. Rev. B **74**, 020101(R) (2006).
[22] H. Béa, M. Bibes, A. Barthélémy, K. Bouzehouane, E. Jacquet, A. Khodan, and J.-P. Contour, S. Fusil, F. Wyczisk, A. Forget, D. Lebeugle, D. Colson, and M. Viret, Appl. Phys. Lett. **87**, 072508 (2005).
[23] W. J. Antel, F. Perjeru, and G. R. Harp, Phys. Rev. Lett. **83**, 1439 (1999).
[24] H. Ohldag, T. J. Regan, J. Stöhr, A. Scholl, F. Nolting, J. Lüning, C. Stamm, S. Anders, and R. L. White, Phys. Rev. Lett. **87**, 247201 (2001).
[25] T. P. A. Hase, B. D. Fulthorpe, S. B. Wilkins, B. K. Tanner, C. H. Marrows, and B. J. Hickey, Appl. Phys. Lett. **79**, 985 (2001).
[26] U. Nowak, A. Misra, and K. D. Usadel, J. Magn. Magn. Mater. **240**, 243 (2002).
[27] L. Sampaio, A. Mougin, J. Ferré, A. Brun, P. Georges, H. Bernas, S. Poppe, T. Mewes, J. Fassbender, and B. Hillebrands, Europhys. Lett. **63**, 819 (2003).
[28] A. P. Malozemoff, Phys. Rev. B **35**, 3679 (1987).
[29] D. Mauri, H. C. Siegmann, P. S. Bagus, and E. Kay, J. Appl. Phys. **62**, 3047 (1987).
[30] T. Ambrose, R. L. Sommer, and C. L. Chien, Phys. Rev. B **56**, 83 (1997).
[31] A. Mougin, J. Borme, R. L. Stamps, A. Marty, P. Bayle-Guillemaud, Y. Samson, and J. Ferre, Phys. Rev. B **73**, 024401 (2006).
[32] T. Mewes, H. Nembach, M. Rickart, S. O. Demokritov, J. Fassbender, and B. Hillebrands, Phys. Rev. B **65**, 224423 (2002).
[33] W. Zhu, L. Seve, R. Sears, B. Sinkovic, and S. S. P. Parkin, Phys. Rev. Lett. **86**, 5389 (2001).
[34] W. Kleemann, Phys. **2**, 105 (2009).